

Optimization of europium transport through a supported liquid membrane containing Cyanex 272 using response surface methodology

P. Zaheri*, F. Zahakifar, M. Gh. Maragheh

Nuclear Fuel Cycle Research School, Nuclear Science and Technology Research Institute, AEOI, P.O. Box: 11365-8486, Tehran-Iran

Received: July 20, 2021; Revised: March 27, 2023

In this study, the transport of europium (Eu^{3+}) was investigated using bis (2,4,4-trimethylpentyl) phosphinic acid (Cyanex 272) extractant in a supported liquid membrane (SLM) system. The effect of various parameters such as feed phase pH, extractant concentration, and stripping phase concentration was investigated with response surface methodology (RSM). At the optimum conditions, membrane permeability of $2.35 \times 10^{-5} \text{ m s}^{-1}$ was obtained. The results demonstrated that the transfer kinetics follow a first-order model. Examination of SLM stability showed that the membrane used was stable for six runs, and permeability did not change significantly. The permeability and stability of the membrane decreased with the increment of the membrane pore size. Examination of the separation of dysprosium (Dy^{3+}) and Eu^{3+} with the Taguchi method showed that feed pH has the most significant effect on the separation factor.

Keywords: Europium; Supported liquid membrane; Permeability; Response surface methodology; Cyanex 272, Separation.

INTRODUCTION

In the last few decades, the applications of rare earth elements have increased, and the demand for them has widely grown. There are numerous applications of these elements in the nuclear, metallurgical, chemical, catalytic, electrical, and magnetic industries. Europium, Eu^{3+} , is a rare earth element that is used to create blue and red light in TVs and computer monitors due to its unique optical properties. Other applications include wireless internet systems, optical fibers, X-ray imaging, fluorescent lamps, and LEDs [1, 2].

Various methods have been used to purify and separate rare earth elements, such as fractional crystallization [3], ion exchange [4], and solvent extraction [5-7]. In recent years, liquid membrane (LM) separation technology has been used as an alternative to conventional solvent extraction methods. This technology has been considered by many researchers due to lower investment and operating costs, lower energy consumption, economical use of expensive extractants, and high selectivity [8, 9].

Mass transfer in the liquid membrane is affected by the shape and structure of the liquid membrane. The liquid membrane is divided into phase dispersion (emulsion liquid membrane) and non-phase dispersion (bulk liquid membrane and supported liquid membrane) methods [10]. A supported liquid membrane is a result of impregnating a porous solid base with a liquid

membrane that contains diluent and extractant. The consumption of extractant in the method of supported liquid membranes is lower than that of emulsion membranes and bulk liquid membranes. Among the various types of supported liquid membranes, the use of flat-sheet supported liquid membrane is one of the simplest ways to evaluate the performance of the liquid membrane method [11].

On one side of the membrane, the reaction between the solute ions and the extractant molecules leads to the formation of a solute-extractant complex. This reaction is reversed on the other side of the membrane, and the solute ions enter the stripping phase. The extractant molecules stay inside the membrane to repeat this cycle [12].

So far, many researchers have used the liquid membrane method to extract rare earth elements. However, this process has not yet reached the industrial stage and still needs to optimize the parameters to improve the efficiency and stability of the system.

Gaikwad scrutinized synergetic transport of europium through a contained supported liquid membrane using trioctylamine and tributyl phosphate as carriers [13]. In another work, the transport of Eu^{3+} through an SLM was investigated using octyl(phenyl)-N,N-diisobutylcarbamoyl-methylphosphine oxide (CMPO) as an extractant. The maximum extraction of Eu^{3+} was achieved by the combination of 0.2 mol L^{-1} CMPO with 5% iso-decanol/n-dodecane at feed acid concentration of

* To whom all correspondence should be sent:
E-mail: pzaheri@aeoi.org.ir

3–4 mol L⁻¹ HNO₃ [14]. Lee *et al.* studied the influence of effective parameters on the permeation of Eu³⁺ using an SLM system containing 2-ethylhexyl phosphonic acid mono-2-ethylhexyl ester (PC-88A) [2]. Liang *et al.* separated the Eu³⁺ up to 95.3% using a dispersion combined liquid membrane (DCLM) in the presence of 2-ethyl hexyl phosphonic acid-mono-2-ethyl hexyl ester (P507) [15]. Eu³⁺ pertraction trend also in the SLM system was determined by N,N,N',N'-tetra-2-ethylhexyl diglycolamide (T2EHDGA) as the extractant. Under optimum conditions, the membrane diffusion coefficient was 4.25×10⁻⁶ cm².s [16].

In this study, for the first time the influence of various parameters on Eu³⁺ transport through a supported liquid membrane (SLM) containing Cyanex 272 was investigated based on design expert statistical analysis software as a new method. The aim of the research was to establish whether the correlations predicted by the software have sufficient accuracy in predicting the Eu³⁺ transport via a SLM. In case of acceptable accuracy, it is possible to save costs related to the consumption of raw materials by conducting fewer tests using this method.

MATERIALS AND METHODS

Materials

To prepare the organic phase, Cyanex 272 (bis (2,4,4-trimethylpentyl) phosphinic acid) as an extractant and kerosene as a diluent were used. The hydrophobic polytetrafluoroethylene (PTFE) membranes used in the present study were procured from Millipore (Billerica, MA, USA). The PTFE membrane was placed inside the organic phase, and a supported liquid membrane (SLM) was prepared.

The feed solution was prepared by dissolving Eu(NO₃)₃.6H₂O and Dy(NO₃)₃.6H₂O in distilled water. The pH of the solutions was adjusted using HNO₃ or NaOH. The stripping phase solutions were prepared by dissolving a certain amount of nitric acid in distilled water. All materials except the PTFE membrane were purchased from Merck (Darmstadt, Germany). All chemicals used were of analytical grade and used without purification.

Apparatuses

The pH of the aqueous solutions was measured using a Sartorius pH meter. The interfacial tension of the phases was measured by the device model Krüss GmbH. The viscosity was measured using an ubbelohde viscometer.

The membrane system consists of two chambers of feed and stripping phases with the same volume of 200 mL. The Plexiglas chambers have no direct

contact with each other and exchange ions with each other only through the membrane. Ion concentrations in the aqueous phase were measured using a UV-Visible spectrophotometer (model Cary 100, Varian, Palo Alto, CA, USA).

To determine the concentration of ions in the aqueous solutions with a UV-Vis device, the procedure provided by Marczenko was used [17]. First, standard solutions were prepared and then the concentration of the desired samples was determined based on the values of the prepared standards.

Experimental procedure

For experiments, the prepared membrane was placed in the membrane system. The speed of the stirrers in the feed and stripping phases was set at 500 rpm. The feed and stripping solutions were sampled at regular intervals. The following equation was used to calculate the experimental permeability coefficient (P) in the membrane [18]:

$$P \frac{A}{V_f} t = \ln \left(\frac{[M^{3+}]_f}{[M^{3+}]_{f,0}} \right) \quad (1)$$

where $[M^{3+}]_{f,0}$ and $[M^{3+}]_f$ are the concentrations of Eu³⁺ ions in the feed at t = 0 and t = t, respectively. A and V_f are the effective membrane area and the feed phase volume, respectively. The value of P under different experimental conditions can be calculated by plotting $\ln([M^{3+}]_f/[M^{3+}]_{f,0})$ versus t. By the values of P and drawing the changes of 1/P with $[H^+]^3$ at a constant concentration of the extractant, the permeability coefficient in the membrane and the mass transfer coefficient at the feed-membrane surface was determined using the following equation [18].

$$\frac{1}{P} = \frac{1}{K_f} + \frac{d_m}{D_{m,c}} \frac{\zeta [H^+]^3}{\epsilon K_e [HR]^3} \quad (2)$$

The parameters K_f, D_{m,c}, d_m, K_e, ε, and ζ are the mass transfer coefficient in the feed phase (m/s), the complex penetration coefficient in the membrane (m/s), the membrane thickness (m), the reaction equilibrium constant (unitless), the membrane porosity, and membrane tortuosity, respectively [19]. In a previous study, the K_e of europium was determined to be 7.58×10⁻⁵ [19]. The following equation was used to calculate the percentage of metal transfer through the membrane:

$$\text{Extraction\%} = \left(\frac{[M^{3+}]_{f,0} - [M^{3+}]_f}{[M^{3+}]_{f,0}} \right) \times 100 \quad (3)$$

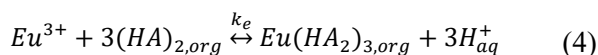
Experimental design

The experiments of Eu transport *via* the SLM are designed utilizing RSM based on the central composite design (CCD) with design expert software. A 2³ CCD with 3 independent variables (feed phase pH, extractant concentration, and stripping phase concentration) was investigated at five different levels (- α , -1, 0, +1, + α) containing 20 experiments [20].

Analysis of variance (ANOVA) was used to analyze the data obtained from the design of experiment and the degree of impact of the main variables, interaction between factors, standard deviation coefficients, etc. Analysis of variance, or ANOVA, is a statistical method that separates observed variance data into different components to use for additional tests [21, 22]. The significance of the coefficients of the model is determined using the F and P-values. P-values less than 0.05 for each factor indicate that it is statistically significant [23].

Mechanism of reaction

In low-polarity organic solvents, organophosphorus extractants are present in the form of a dimer (HA)₂. Therefore, the extraction reaction can be considered as follows [1]:



In this mechanism, Eu³⁺ ions are transferred from the feed phase to the recovery (stripping) phase, and the protons move in the opposite direction. The driving force for this transfer mechanism is the concentration gradient of protons. Therefore, ions pass from the feed phase to the recovery phase in the opposite direction of their concentration gradient. This condition occurs when the concentration of protons in the recovery phase is much higher than in the feed phase.

RESULTS AND DISCUSSION

Study of interfacial tension of organic and aqueous phases

Fig. 1 shows the interfacial tension of distilled water and of the organic phase of the membrane as a function of the concentration of Cyanex 272 extractant in the kerosene. The results show that the surface tension decreases on increasing the extractant concentration in the organic phase. Therefore, the extractants show surface activity in kerosene. A decrease in interfacial tension is observed in three areas: a gentle slope at low extractant concentrations (region 1), then an almost sharp slope at reduced interfacial tension (region 2),

and finally, nearly zero slope at high extractant concentrations (region 3). The decrease in interfacial tension is due to the adsorption of the extractant molecules. The Gibbs relation expresses it [24]:

$$\Gamma = -\frac{d\gamma}{RT \, d \ln a} \quad (5)$$

where Γ , γ , a , and R are the surface accumulation density (mol m⁻²), interfacial tension (N m⁻¹), the surface activity of the adsorbed components in the organic phase (mol L⁻¹), and the universal gas constant (J K⁻¹ mol⁻¹), respectively.

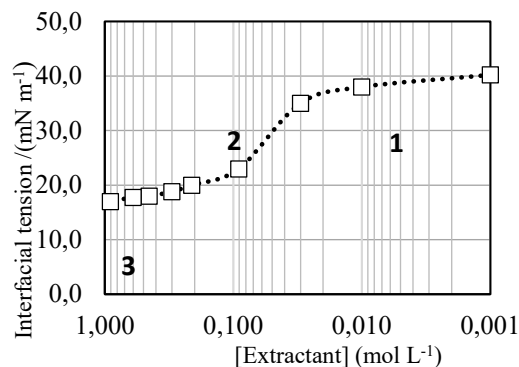


Fig. 1. Interfacial tension of organic phase and aqueous phase at different concentrations of the extractant

Fig. 2 shows the changes in the interfacial tension of the organic and aqueous phases as a function of the Eu³⁺ concentration in the aqueous phase. When the liquid membrane phase is in contact with an aqueous solution (containing metal ions), the interfacial tension changes due to the formation of complex molecules on the surface. Since the formed complexes have different surface activities, at a low concentration of extractant (0.03 mol L⁻¹), the interfacial tension increases with the increasing concentration of europium ions.

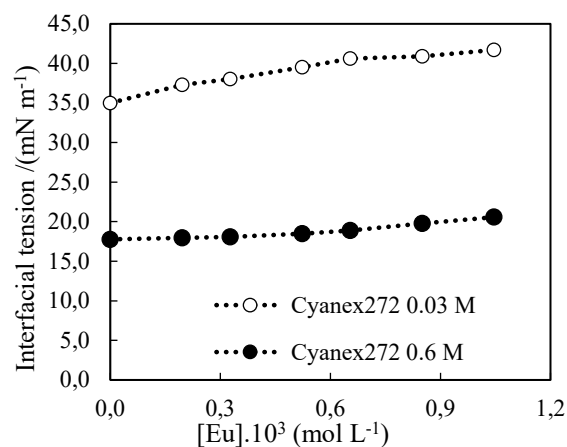


Fig. 2. Interfacial tension of organic phase and aqueous phase with different concentrations of Eu³⁺

In other words, the formed complexes have lower surface activity than free extractant molecules due to their low tendency to form hydrogen bonds with water molecules.

As a result, the concentration of complexes formed on the surface increases with increasing the concentration of Eu^{3+} ions. So, interfacial tension also increases. This increase continues until all the extractant molecules on the surface form complexes with Eu^{3+} ions. At high concentrations of the extractant (0.6 mol L^{-1}), the increase in interfacial tension with increasing concentrations of metal ions is negligible.

Study of parameters affecting Eu^{3+} transfer with RSM

The effect of feed phase pH, extractant concentration and stripping phase concentration was

Table 1. The levels of effective parameters and the results of membrane permeability tests for Eu^{3+} transfer using RSM.

Run	Feed phase pH	Extractant concentration (mol L ⁻¹)	Stripping phase concentration (mol L ⁻¹)	Eu^{3+} permeability $\times 10^5 \text{ (m s}^{-1}\text{)}$ (Experimental)	Eu^{3+} permeability $\times 10^5 \text{ (m s}^{-1}\text{)}$ (Model predicted)
1	3.25	0.10	1.75	0.33	0.33
2	1.61	0.26	2.49	0.40	0.39
3	1.61	0.74	2.49	0.77	0.86
4	0.50	0.50	1.75	0.70	0.71
5	3.25	0.50	1.75	1.14	1.16
6	3.25	0.50	3.00	0.98	1.01
7	1.61	0.74	1.01	1.20	1.02
8	4.89	0.26	1.01	1.32	1.26
9	3.25	0.50	1.75	1.27	1.16
10	3.25	0.50	0.50	1.02	1.32
11	4.89	0.74	2.49	1.67	1.53
12	3.25	0.90	1.75	0.88	0.94
13	3.25	0.50	1.75	1.17	1.16
14	3.25	0.50	1.75	1.16	1.16
15	6.00	0.50	1.75	2.18	2.28
16	1.61	0.26	1.01	0.48	0.48
17	4.89	0.26	2.49	1.07	1.07
18	3.25	0.50	1.75	1.25	1.16
19	3.25	0.50	1.75	1.19	1.16
20	4.89	0.74	1.01	1.88	1.77

Table 2. Results of ANOVA for Eu^{3+} transfer data

Source	Sum of squares	df	Mean square	F value	p-value
Model	0.35	6	0.058	68.35	<0.0001
pH (A)	0.17	1	0.17	203.69	<0.0001
Ex. Con. (B)	0.85	1	0.085	100.80	<0.0001
Str. Con. (C)	0.0089	1	0.0089	10.57	0.063
AB	0.0037	1	0.0037	4.42	0.0555
A ²	0.0039	1	0.0039	4.72	0.0490
B ²	0.069	1	0.069	81.61	<0.0001
Residual	0.01	13	0.0008		

investigated using RSM. The results are presented in Table 1. The permeability of Eu^{3+} was the response of the experiments. Experiments 5, 9, 13, 14, 18, and 19 have the same test condition, which indicates the appropriate repeatability of the experiments. The proposed model also provides the predicted results.

Analysis of variance. Analysis of variance (ANOVA) was used to analyze the data and determine the effect of the main parameters, the interaction between them, and the standard deviation coefficients. The results showed that the quadratic model is the best model for fitting the data obtained from the experiments. The results of ANOVA for the proposed regression model are reported in Table 2. Values of P less than 0.05 for each expression indicate that it is statistically significant.

The quadratic model for Eu^{3+} transfer via SLM containing Cyanex 272 is as follows:

$$P \times 10^5 = \left(\begin{array}{c} 0.387 + 0.056pH + 1.727Ex - \\ 0.034 Str - 0.055pH * Ex + 0.0062pH^2 \\ -1.215 Ex^2 \end{array} \right)^{0.33}$$

The F-value for the model is equal to 31.83, which indicates the model validity. The coefficient of determination (R-squared) and the adjusted R-squared were 0.98 and 0.96, respectively. Therefore, the experimental data and the model predictions are very well matched. A comparison of experimental data with the statistical model provided by the software is presented in Fig. 3. It can be observed that the predicted values are very close to the experimental values.

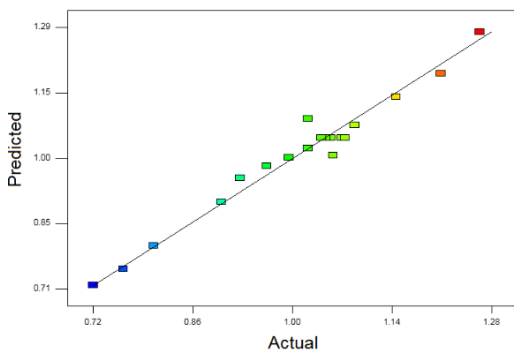


Fig. 3. Comparison of experimental data with the statistical model

The graph of the residuals versus the experimental data is shown in Fig. S1. It is observed that the resulting chart has a random trend and does not follow a specific pattern. Therefore, there are no latent variables and no systematic errors.

Study of the effect of parameters with RSM

The influence of effective parameters on Eu^{3+} transfer is shown in Figs. 4(a) to (c). As Eu^{3+} ions move from the feed to the stripping phase, the protons move in the opposite direction. The concentration gradient of protons is the driving force for the transfer of Eu^{3+} ions. Therefore, the acidity of the feed phase affects the transfer. The impact of feed phase pH in the range of 0.5 to 6 on the Eu^{3+} transfer was investigated. The results showed that by increasing the pH of the feed phase to 5, the penetration of Eu^{3+} increases. With the increment of pH of the feed phase, the rate of complex formation at the boundary of the feed phase and liquid membrane phase increases. As a result, a higher concentration gradient of the complex increases the penetration of Eu^{3+} via the membrane [25].

At lower pH values, the concentration of H^+ ions at the membrane boundary is higher than that of Eu^{3+} ions. As a result, competition with metal ions occurs at the interface of the feed and liquid membrane phase. Therefore, the transfer of metal ions is reduced [26].

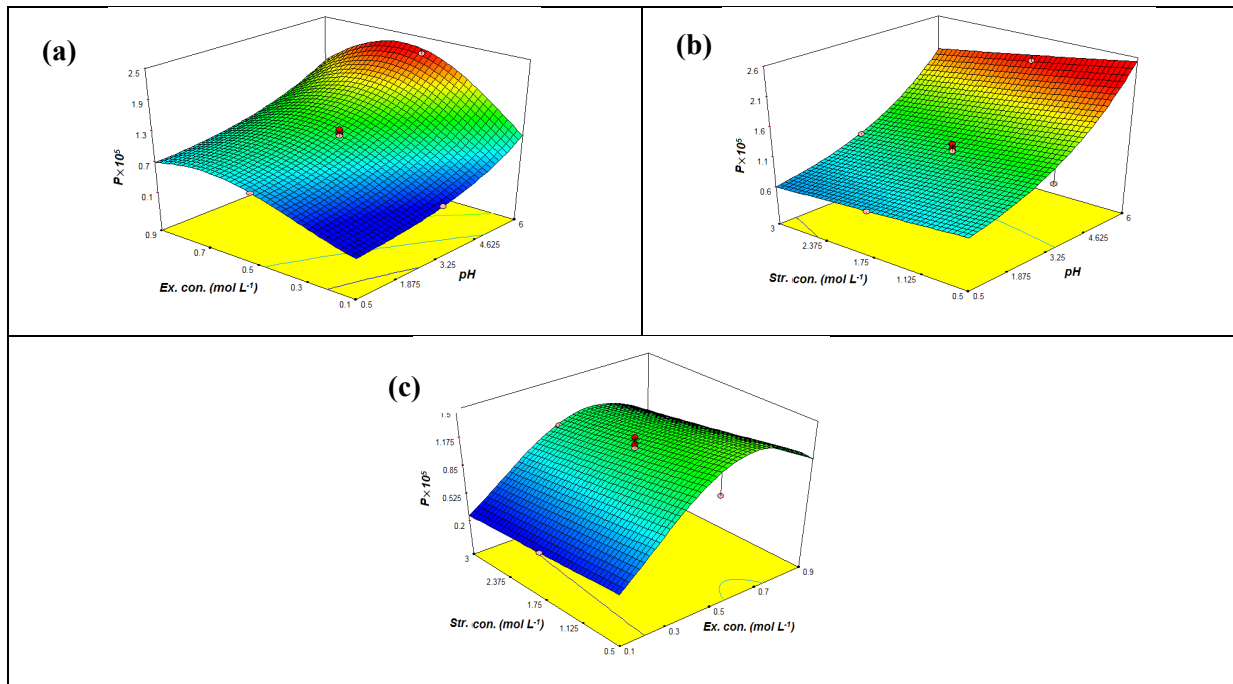


Fig. 4. Influence of effective parameters on membrane permeability for Eu^{3+} transfer. a) feed phase pH and extractant concentration; b) feed phase pH and stripping phase concentration; and c) stripping phase concentration and extractant concentration

The effect of stripping phase concentration (0.5-3 mol L⁻¹) was also investigated. According to Eq. 2, the driving force for the transfer of Eu³⁺ increases with increasing HNO₃ concentration in the stripping phase. As a result, the permeability of the membrane increases. The membrane permeability slightly decreases with an increase in the HNO₃ concentration to 3 mol L⁻¹. In this case, the concentration of protons at the interface between the liquid membrane and the stripping phase increases. Some extractant molecules react with the protons at the interface between the liquid membrane and the stripping phase. As a result, the membrane permeability is reduced [21]. Increasing the acid concentration in the stripping phase reduces the interfacial tension between the liquid membrane phase and the aqueous phase and favors the dissolution of the extractant in the aqueous phase [22]. Also, the high contact time between the acidic aqueous solution and the membrane phase causes gradual degradation of the latter.

In investigating the effect of extractant concentration on Eu³⁺ penetration, the maximum value obtained in these diagrams can be explained by the change in the viscosity of the liquid membrane. In the first part of the diagram, the higher concentration of the extractant increases the Eu³⁺-extractant complex concentration. So, the membrane permeability increases. On the other hand, the viscosity of the liquid membrane phase increases with the extractant concentration increment, which lowers the penetration of complexes *via* the liquid membrane [10]. Changes in the viscosity of the liquid membrane are shown in Fig. 5. According to experimental data, there is an exponential relationship between viscosity and extractant concentration, which is expressed as follows:

$$\mu = \alpha \exp(\beta C) \tag{7}$$

The constant values of α and β are 1.4943 and 0.7702, respectively. The diffusion coefficient of the

complex in the liquid membrane with increasing extractant concentration was calculated by Eq. 2 and is reported in Table 3. As can be observed, the diffusion coefficient decreases with increasing extractant concentration.

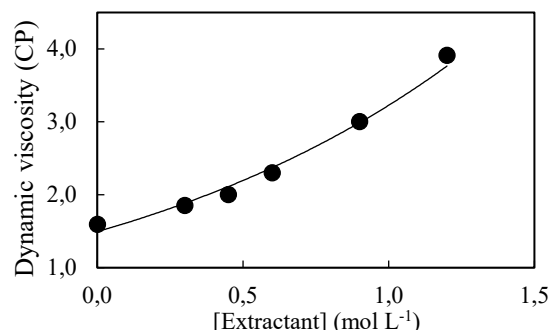


Fig. 5. Influence of extractant concentration on the liquid membrane viscosity.

Table 3. Influence of extractant concentration on the diffusion coefficient of the complexes in the liquid membrane.

$D_{m,c}$ (m ² s ⁻¹)	Cyanex272 concentration (mol L ⁻¹)
1.51×10^{-9}	0.1
7.33×10^{-10}	0.3
3.05×10^{-10}	0.6
5.42×10^{-10}	0.9

Validation of the proposed model. ANOVA showed that the model is well consistent with the data. For model validation, the experimental conditions of the parameters were randomly selected, and the experiment was performed. Then the obtained results were compared with the values predicted by the model. The error values in Table 4 show that the model has well predicted the experimental results.

The design-expert software predicts that at pH=6, [HNO₃] = 0.1 mol L⁻¹, and [Cyanex 272] = 0.57 mol L⁻¹, maximum permeability (2.47×10^{-5} m s⁻¹) can be expected. Under optimum conditions, experimental permeability was obtained at 2.35×10^{-5} m s⁻¹.

Table 4. Validation of the Eu³⁺ transfer model using random experiments.

Run	Feed phase pH	Extractant concentration (mol L ⁻¹)	Stripping phase concentration (mol L ⁻¹)	Predicted Eu ³⁺ permeability $\times 10^5$ (m s ⁻¹)	Experimental Eu ³⁺ permeability $\times 10^5$ (m s ⁻¹)	Error (%)
1	0.8	0.25	1	0.38	0.35	8.10
2	1.5	0.8	2	0.85	0.90	4.17
3	2.7	0.5	0.8	1.14	1.09	5.10
4	3.5	0.7	2.5	1.18	1.26	5.98
5	4.7	0.4	1.5	1.50	1.53	2.11
Optimum point	6	0.57	1	2.47	2.35	5.38

Study of the effect of membrane pore size

To study the effect of membrane pore size on permeability, PTFE supports with pore sizes of 0.22, 0.45, 1, and 5 μm , porosity of 85%, and uniform thickness (150 μm) were examined. The results in Fig. 6 show that the permeability and stability of the membrane decreased with the increment of membrane pore size. This trend indicates that larger pores have lower ability to hold the liquid membrane [27].

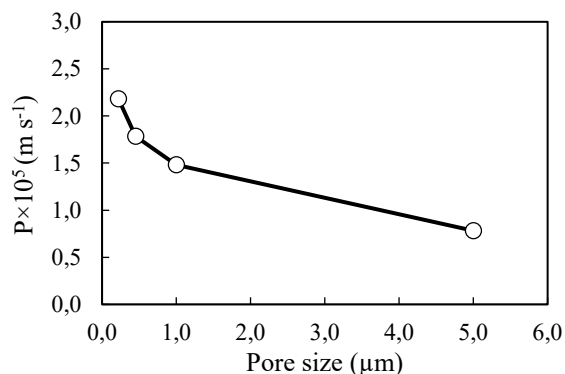


Fig. 6. Effect of the membrane pore size on the permeability ($[\text{Eu}] = 0.61 \times 10^{-3} \text{ mol L}^{-1}$, $[\text{Cyanex 272}] = 0.6 \text{ mol L}^{-1}$, $\text{pH} = 6$).

Therefore, on increasing the size of the pores, the exit of the liquid membrane from the pores of the support becomes faster and causes instability.

Reaction kinetics

The highest permeability occurs at the extractant concentration of 0.57 mol L^{-1} , stripping concentration of 1 mol L^{-1} , and $\text{pH} = 6$. The concentration-time diagram under these conditions ($[\text{Eu}] = 0.61 \times 10^{-3} \text{ mol L}^{-1}$), is shown in Fig. 7. The results showed that the increasing trend in the stripping phase is approximately equal to the decrement trend in the feed phase. Therefore, the accumulation of Eu^{3+} ions in the liquid membrane phase is negligible.

Fig. 8 shows the changes in $\ln(C/C_0)$ versus time. As observed, there is a linear relationship between them. Therefore, the transfer of Eu^{3+} ions via the SLM using the Cyanex 272 extractant has first-order kinetics.

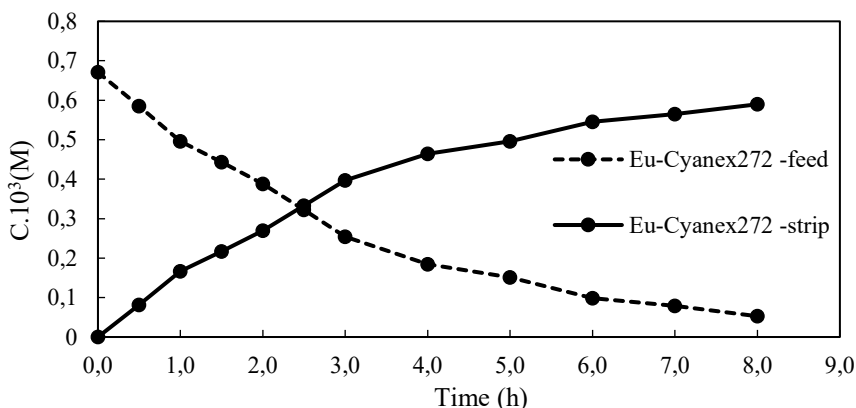


Fig. 7. Changes in Eu^{3+} concentration versus time under optimal conditions.

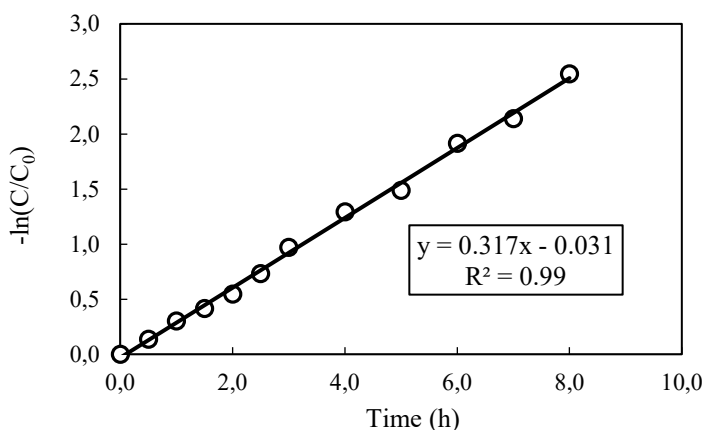


Fig. 8. Kinetics of Eu^{3+} transfer under optimal conditions.

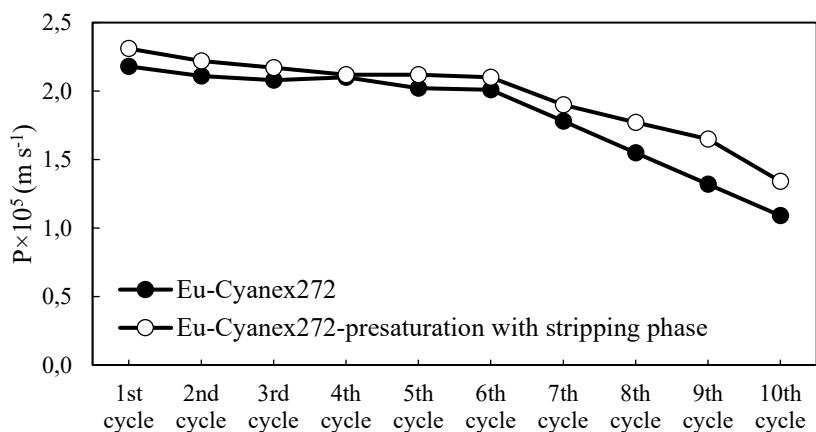


Fig. 9. SLM stability and effect of saturation of the liquid membrane and stripping phases on it.

Table 5. Previous studies on the extraction of Eu³⁺ using liquid membranes.

Extractant	Diluent	Stripping agent	Method	Extraction %	Stability	Ref.
D2EHPA	Kerosene	HNO ₃	SDLM	94.2%	N/A	[30]
T2EHDGA	n-Dodecane	HNO ₃	SLM	95.0%	20 days	[31]
PC-88A	Kerosene	HCl	SLM	N/A	N/A	[2]
P507	Kerosene	HCl	DCLM	95.3%	N/A	[15]
TOA + TBP	Kerosene	N/A	CSLM	N/A	50 h	[13]
D2EHPA+Cyanex 272	Kerosene	HNO ₃	SLM	96.0%	9 days	[12]
Cyanex 272	Kerosene	HNO ₃	SLM	92.3%	6 days	This work

Evaluation of SLM stability

For evaluating the stability of the used SLM, ten consecutive experiments were done with one support. The experiment duration was 4 h, and after each run, feed and stripping phase solutions were replaced with fresh ones. The results are shown in Fig. 9. After six runs, the permeability did not decrease significantly.

The solubility of the organic and aqueous phases (especially that of the stripping phase) is one of the main causes of SLM instability [28]. The organic and stripping phases were saturated before use in the SLM to study this effect. The results showed that saturation improves the stability of the membrane.

After five days and a reduction of membrane permeability, to compensate for the lost liquid membrane phase, the polymer support of the membrane was again immersed in the organic phase for 24 h and reused. The results showed that the membrane permeability is 1.75 m² s⁻¹, and its value is less than in the first cycle. Zang *et al.* stated that the reason for this decrement was the increase in the pore size due to its continuous use [29]. A summary of previous studies for the extraction of Eu³⁺ using liquid membranes and their stability is presented in Table 5. A comparison of the results shows that the

presence of Cyanex 272 in the LM provides stability and Eu³⁺ extraction in the range of reported studies.

Separation of Dy and Eu³⁺ by Taguchi method

Dysprosium is an element that is commonly found with europium. Due to the similar chemical properties of Dy and Eu, the separation of these elements is significant [32, 33]. In this section of the experiments, the separation of dysprosium and europium was investigated. Taguchi method was used to study the effect of different parameters on the separation factor (SF). Optimization of the separation factor was performed using Qualitek-4 software. The studied factors included the ratio of metal ions concentrations in the feed phase, extractant concentration in the membrane phase, feed phase pH, and stripping phase concentration. To minimize the error of the experimental results, the experiments were repeated, and the mean separation factor (SF) was calculated. The separation factor of dysprosium and europium was calculated from the following equation:

$$SF(Dy/Eu) = \frac{([Dy]/[Eu])_{strip}}{([Dy]/[Eu])_{feed,t=0}} \quad (8)$$

Table 6. Parameters, levels and separation factors (SF) of Dy and Eu

Run	pH _f (A)	[HNO ₃] (B)	[Cyanex272] (C)	[Dy]/[Eu] (D)	SF (Dy/Eu) (Y)
1	0.5	0.5	0.3	0.5	2.57
2	0.5	1	0.45	1	2.80
3	0.5	2	0.6	2	1.61
4	2	0.5	0.45	2	1.88
5	2	1	0.6	0.5	1.09
6	2	2	0.3	1	1.21
7	4	0.5	0.6	1	1.40
8	4	1	0.3	2	1.29
9	4	2	0.45	0.5	1.04

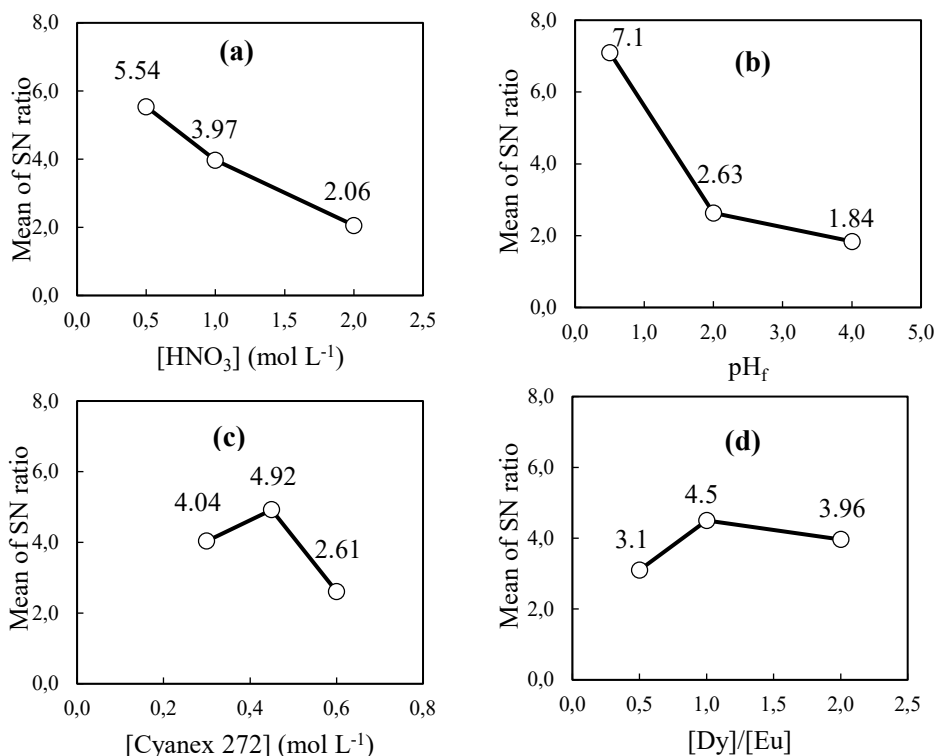


Fig. 10. Effect of a) stripping phase concentration; b) feed phase pH; c) extractant concentration in the membrane phase and d) ratio of metal ions concentrations in feed on the SF of Dy and Eu

The parameters, levels, and SFs of Dy and Eu³⁺ are presented in Table 6. The tool that the Taguchi design method uses to analyze the results is the signal/noise (SN) ratio. Fig. 10 shows the changes in the SN ratio at different levels of factors affecting the SF. In Fig. 10, higher SN values indicate a more significant SF. The results predict that at pH=0.5, [HNO₃]=0.5 M, [Cyanex 272] = 0.45 mol L⁻¹ and Dy/Eu=1, a maximum separation factor (3.02) can be expected. Under these conditions, a validation test was repeated, and SF=2.73 was obtained. Analysis of variance (ANOVA) showed that the most important factor influencing the SF of Dy and Eu³⁺ is the pH of the feed phase. On the other hand, based on the hard and soft acid-base (HSAB) theory [34], the low pH of the solution favors the nature of the

Cyanex 272 molecules, and therefore the Dy ions have a stronger tendency to interact with them.

CONCLUSIONS

In this paper, a SLM system was used for the transport of Eu³⁺ using Cyanex 272 extractant. The effect of parameters such as feed phase pH, extractant concentration, and stripping phase concentration were studied with RSM. A quadratic model was proposed that was in good agreement with the experimental data. The results showed that the feed phase pH and Cyanex 272 concentration were the effective parameters in the Eu³⁺ transfer through the SLM. The kinetic studies also verified the first-order model for transferring of Eu³⁺ ions.

Membrane permeability of 2.35×10⁻⁵ m s⁻¹ was obtained with 0.57 mol L⁻¹ Cyanex 272, pH = 6, and

stripping phase concentration of 1 mol L⁻¹. At these optimum conditions, the membrane was suitably stable for six runs. However, the stability and hence, the permeability of the membrane decreased with the increment of membrane pore size.

The maximum separation factor (SF = 2.73) of Dy³⁺ and Eu³⁺ was obtained at pH = 0.5, [HNO₃] = 0.5 mol L⁻¹, [Cyanex 272] = 0.45 mol L⁻¹, and Dy³⁺/Eu³⁺ = 1.

REFERENCES

1. N. Krishnamurthy, C. K. Gupta, Extractive metallurgy of rare earths. CRC press, 2015.
2. C.-J. Lee, B.-R. Yang, *The Chemical Engineering Journal and The Biochemical Engineering Journal*, **57** (3), 253 (1995).
3. S. Wu et al., *Chemical Engineering Journal*, **335**, 774 (2018).
4. G. Saipriya, R. Kumaresan, P. K. Nayak, K. A. Venkatesan, M. P. Antony, T. Kumar, *Journal of Radioanalytical and Nuclear Chemistry*, **314** (3), 2557 (2017).
5. R. Banda, F. Forte, B. Onghena, K. Binnemans, *RSC Advances*, **9** (9), 4876 (2019).
6. B. B. Mishra, N. Devi, *Journal of Molecular Liquids*, 271, 89 (2018).
7. P. Ren et al., *Inorganic Chemistry*, **59** (19), 14218 (2020).
8. F. Zahakifar, A. Charkhi, M. Torab-Mostaedi, R. Davarkhah, *Radiochimica Acta*, **106** (3), 181 (2018).
9. F. Zahakifar, A. Charkhi, M. Torab-Mostaedi, R. Davarkhah, *Journal of Radioanalytical and Nuclear Chemistry*, **316** (1), 247 (2018).
10. V. S. Kislik, Liquid membranes: principles and applications in chemical separations and wastewater treatment. Elsevier, 2009.
11. P. Zaheri, T. Mohammadi, H. Abolghasemi, M. Ghannadi Maraghe, *Chemical Engineering Research and Design*, **100**, 81 (2015).
12. P. Zaheri, H. Abolghasemi, M. G. Maraghe, T. Mohammadi, *Chemical Engineering and Processing: Process Intensification*, **92**, 18 (2015).
13. A. G. Gaikwad, *Talanta*, **63** (4), 917 (2004).
14. R. Kumar, S. A. Ansari, P. Kandwal, P. K. Mohapatra, *Chemical Engineering Research and Design*, **168**, 307 (2021).
15. P. Liang, W. Liming, F. Xinglong, *Chinese Journal of Chemical Engineering*, **19** (1), 33 (2011).
16. S. Panja, P. K. Mohapatra, S. K. Misra, S. C. Tripathi, *Separation Science and Technology*, **46** (12), 1941 (2011).
17. Z. Marczenko, M. Balcerzak, Separation, preconcentration and spectrophotometry in inorganic analysis, Elsevier, 2000.
18. P. Zaheri, H. Abolghasemi, T. Mohammadi, M. G. Maraghe, *Chemical Papers*, **69** (2), 279 (2015).
19. P. Zaheri, H. Ghassabzadeh, H. Abolghasemi, M. G. Maraghe, T. Mohammadi, *The Canadian Journal of Chemical Engineering*, **95** (3), 524 (2017).
20. F. Zahakifar, A. Keshtkar, E. Z. Souderjani, M. Moosavian, *Progress in Nuclear Energy*, **124**, 103335 (2020).
21. M. R. A. Shadbad, P. Zaheri, H. Abolghasemi, F. Zahakifar, *Chemical Engineering and Processing-Process Intensification*, 109268 (2023).
22. F. Zahakifar, A. Charkhi, M. Torab-Mostaedi, R. Davarkhah, A. Yadollahi, *Journal of Radioanalytical and Nuclear Chemistry*, 1 (2018).
23. H. Arabi, S. Milani, H. Abolghasemi, F. Zahakifar, *Journal of Radioanalytical and Nuclear Chemistry*, **327**, 653 (2021).
24. J. Zhao, X. Sun, W. Li, S. Meng, D. Li, *Journal of Colloid and Interface Science*, **294** (2), 429 (2006).
25. M. Hasan, R. Aglan, S. El-Reefy, *Journal of Hazardous Materials*, **166** (2-3), 1076 (2009).
26. K. Chitra, A. Gaikwad, G. Surender, A. Damodaran, *Journal of Membrane Science*, **125** (2), 257 (1997).
27. X. Yang, A. Fane, *Journal of Membrane Science*, **156** (2), 251 (1999).
28. M. C. Wijers, M. Jin, M. Wessling, H. Strathmann, *Journal of Membrane Science*, **147**(1), 117 (1996).
29. H.-D. Zheng, B.-Y. Wang, Y.-X. Wu, Q.-L. Ren, *Colloids and Surfaces A: Physicochemical and Engineering Aspects*, **351** (1-3), 38 (2009).
30. P. Liang, W. Liming, Y. Guoqiang, *Journal of Rare Earths*, **29** (1), 7 (2011).
31. S. Panja, P. Mohapatra, S. Misra, S. Tripathi, *Separation Science and Technology*, **46** (12), 1941 (2011).
32. P. Zaheri, H. Abolghasemi, T. Mohammadi, M. G. Maraghe, *Korean Journal of Chemical Engineering*, **32** (8), 642 (2015).
33. M. Mallah, F. Shemirani, M. Ghannadi Maragheh, *Journal of Radioanalytical and Nuclear Chemistry*, **278** (1), 97 (2008).
34. J. E. Huheey, E. A. Keiter, R. L. Keiter, O. K. Medhi, Inorganic chemistry: principles of structure and reactivity. Pearson Education India, 2006.